Weierstraß-Institut
für Angewandte Analysis und Stochastik

im Forschungsverbund Berlin e.V.

Preprint ISSN 0946 – 8633

Effect of higher-order dispersion on modulation instability, soliton propagation and pulse splitting

Ayhan Demircan, Monika Pietrzyk, Uwe Bandelow

submitted: 21st August 2007

Weierstrass Institute for Applied Analysis and Stochastics
Mohrenstraße 39, D-10117 Berlin, Germany
E-Mail: demircan@wias-berlin.de

No. 1249
Berlin 2007

1991 *Mathematics Subject Classification.* 35Q55, 35Q60, 78A60.

Key words and phrases. Modulation instability, nonlinear fibers, pulse splitting, third-order dispersion.

Supported by the DFG Research Center MATHEON "Mathematics for key technologies" in Berlin.

Edited by
Weierstraß-Institut für Angewandte Analysis und Stochastik (WIAS)
Mohrenstraße 39
10117 Berlin
Germany

Fax: + 49 30 2044975
E-Mail: preprint@wias-berlin.de
World Wide Web: http://www.wias-berlin.de/

Abstract

By solving numerically the extended nonlinear Schrödinger equation we investigate the influence of higher-order dispersion effects on the propagation of optical pulses in highly nonlinear fibers. In the anomalous dispersion regime third-order dispersion can, in general, induce soliton fission and yields asymmetric spectra, whereas modulation instability can be slightly suppressed. In the normal dispersion regime we demonstrate pulse splitting by third-order dispersion, as well as its later suppression by fourth-order dispersion.

Key words: modulation instability, nonlinear fibers, pulse splitting, third-order dispersion

1 Introduction

The propagation of a pulse through a nonlinear, dispersive optical medium can result in considerable changes to its temporal and spectral properties, due to interplay of different physical effects acting on the pulse. For example the supercontinuum generation in nonlinear fibers has been a subject of numerous investigations for years, see e.g. the review [1], both because of many applications of supercontinuum sources, as well as of the interesting nonlinear physics that is involved in the spectral broadening process. There is a variety of effects modifying the shape of a pulse and its spectrum, like soliton fission (SF), associated with the generation of dispersive waves [3], modulation instability (MI) [2], Raman scattering, and other four-wave-mixing processes. This situation makes it particularly difficult to identify the impact of each physical process in a specific physical experiment. However, in the anomalous dispersion regime SF and MI, which are described solely by the fundamental nonlinear Schrödinger equation (NLSE) with some perturbation, turn out to be the basic mechanisms. This reflects how inherent properties of the NLSE are of primary importance for the propagation dynamics, even for ultrashort pulse propagation in photonic-crystal fibers (PCF) with extremely high nonlinearity.
To avoid the influence of MI and soliton effects such as SF and self-frequency shift, the pump pulse can be injected within the normal dispersion regime, far from the zero-dispersion wavelength (ZDW). This enables one to investigate the effects of Raman-scattering. In addition, the normal dispersion regime provides parameter regions where the efficiency of four-wave mixing is reduced and the signature of a discrete Raman cascade can be clearly identified. Also the role of cross-phase modulation and parametric four-wave-mixing can be investigated [4, 5]. But fundamental

propagation properties described by the NLSE are suppressed or superimposed by higher-order effects, so that it becomes difficult to isolate the relative contributions of the involved physical parameters.
To investigate the effect of dispersion on the propagation dynamics, we have solved numerically the one-dimensional nonlinear Schrödinger equation for the slowly varying complex envelope $A(z,\tau)$ of a pulse which propagates along the z-axis within a retarded time frame $\tau = t - z/v_g$ with the group velocity v_g:

$$\frac{\partial A}{\partial z} = -\frac{i}{2}\beta_2\frac{\partial^2 A}{\partial \tau^2} + \frac{1}{6}\beta_3\frac{\partial^3 A}{\partial \tau^3} + \frac{i}{24}\beta_4\frac{\partial^4 A}{\partial \tau^4} + i\gamma|A|^2 A \qquad (1)$$

with third-order dispersion (TOD) $\sim \beta_3$ and fourth-order dispersion (FOD) $\sim \beta_4$ in addition. We exclude in our numerical investigations any contribution from phase-matched parametric four-wave mixing and from higher-order nonlinearities as Raman scattering or self-steepening. This corresponds to the situation of a highly nonlinear fiber (HNLF), with pulse durations exceeding several picoseconds and small input powers so that the spectral bandwidth is much smaller than the Raman frequency shift in fused silica, hence the pump pulses do not suffer significantly from intrapulse Raman scattering as in the femtosecond case. Our technique for solving Eq. (1) is based on a standard de-aliased pseudospectral method in which the dispersion parts are calculated in the frequency domain and the nonlinearity is calculated as a product in the time domain. The integration is performed for the whole equation in the frequency domain with an eigth-order Runge-Kutta integration scheme with adaptive stepsize control [6].
Based on that, we demonstrate how strongly even small dispersive effects can affect the propagation dynamics in both the anomalous and in the normal dispersion regime. In the *anomalous* dispersion regime we show how higher-order dispersion influences the MI and the propagation of higher-order solitons. In particular we demonstrate that the TOD can not be neglected for the pulse-MI (c.f. [8]), that it leads to an asymmetry of the spectrum and later on to a subsequent suppression of the MI. The asymmetric perturbation of a higher-order soliton by the TOD does not lead inevitably to its fission. Depending on a critical value of TOD a bound higher-order soliton can still exist and propagate with a modified velocity.
In the *normal* dispersion regime the impact of TOD is even stronger, because the dispersion profile can merge with the anomalous dispersion regime. Then, already a small TOD can lead to a pulse-breakup above a critical pulse power. The splitting is followed by an expansion of the spectrum towards longer wavelengths with the evolution of a broad Stokes component and without any impact of Raman scattering. The Stokes frequency depends strongly on the third-order dispersion coefficient, which enables the transfer of energy to a broad range of longer wavelengths.

2 Anomalous dispersion regime

Propagation of pulses in the anomalous dispersion regime is mainly determined by soliton effects and the modulation instability [8]. An input pulse with a hyperbolic-

secant shape, which we use throughout this paper:

$$A(0,\tau) = A_0 sech(\tau/\tau_0)\,,$$

where τ_0 corresponds to the width of the pulse and the pulse peak power P_0 satifies $P_0 = |A_0|^2$, together with the fiber parameters for the NLSE imply the formation of a higher-order soliton of order N:

$$N^2 \;=\; \frac{\gamma P_0 \tau_0^2}{|\beta_2|}\,.$$

The propagation of a bounded higher-order soliton $N > 1$ is periodic in z with the period $z_0 = \pi\tau_0^2/(2|\beta_2|)$. Accordingly, the soliton period is independent of the peak power and proportional to the dispersion length. However, depending on the width of the input pulse, one observes different behaviors for the same soliton number. Especially the impact of the MI becomes increasingly important with increasing P_0 or a decreasing $|\beta_2|$ [2].

2.1 Higher-order dispersion and modulation instability

The MI refers to a process in which a weak perturbation of a continuous wave (cw) grows exponentially in the form of amplitude modulation. Following the perturbation analysis in [7] the dispersion relation for the modulation wave number K and modulation wave frequency Ω is given as

$$K = \frac{\beta_3\Omega^3}{3} \pm \left[\left(\frac{\beta_2\Omega^2}{2} + \frac{\beta_4\Omega^4}{24}\right)\left(\frac{\beta_2\Omega^2}{2} + \frac{\beta_4\Omega^4}{24} + 2\gamma P_0\right)\right]^{\frac{1}{2}} \tag{2}$$

leading to a MI gain

$$g(\Omega) = Im\left[\left(\frac{\beta_2\Omega^2}{2} + \frac{\beta_4\Omega^4}{24}\right)\left(\frac{\beta_2\Omega^2}{2} + \frac{\beta_4\Omega^4}{24} + 2\gamma P_0\right)\right]^{\frac{1}{2}}\,. \tag{3}$$

For $\beta_4 = 0$, in the anomalous regime, K becomes complex for frequencies $\Omega < \Omega_c = 2N/\tau_0$. Because the MI bandwidth increases as $|\beta_2|$ decreases, the effect of MI becomes very strong in the vicinity of ZDW or for high input powers. Compared to cw the case of a pump-pulse is more complicated, because the MI is superimposed by the the evolution of a soliton, which is usually of higher-order [8, 2]. The main difference between the cw MI and the pulse MI is that the shape of the pump pulse plays an important role in the generation of the modulation ripples. The modulation wavelength of the MI ripples has to be much smaller than the pulse width, so that the center of the pump pulse can be regarded as a relatively flat plateau and the perturbation in form of amplitude modulation can grow at the center. For short pulse widths the MI can be suppressed. But an increase of the pump pulse leads to a decrease of the modulation wavelength and the MI can affect the propagation of the pulse even for extremely short pulses [2].

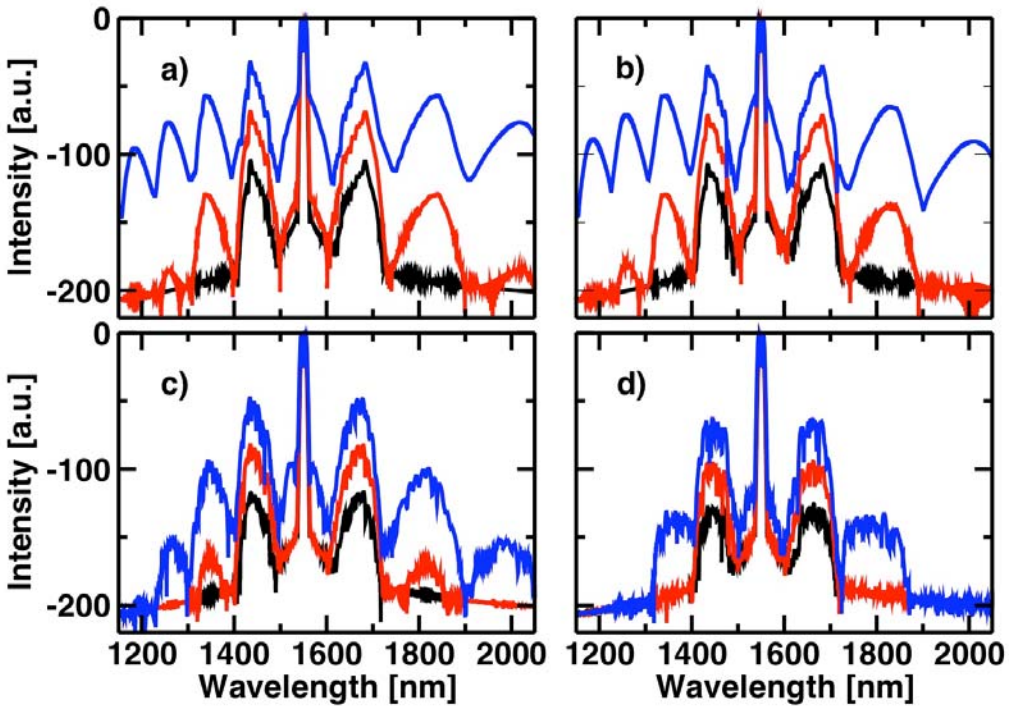

Figure 1: Spectra for the propagation of an input pulse with $P_0 = 0.4kW$ and $\tau_0 = 5ps$ along a fiber with $\beta_2 = -1ps^2/km$, $\gamma = 10.5W^{-1}km^{-1}$ after $z = 6m$ (black), $z = 7m$ (red) and $z = 8m$ (blue) and increasing TOD: a) $\beta_3 = 0$, b) $\beta_3 = 0.01ps^3/km$, c) $\beta_3 = 0.05ps^3/km$ and d) $\beta_3 = 0.1ps^3/km$.

Another important fact of the pulse MI is that TOD (via β_3) has now to be taken into account, which is often neglected. The parameter β_3 has no influence on the modulation frequency in the presence of MI-gain (Eq. 3), but the shape of the pulse is affected by β_3 and therefore also the effect of the MI on the propagation dynamics. Fig. 1 shows the evolution of pulse-spectra experiencing MI along z for increasing values of β_3, indicating that the MI is suppressed with increasing TOD. The spectral evolution without β_3 is shown in Fig. 1a) for comparison. The MI leads to the generation of a Stokes and an anti-Stokes component at Ω_c at $z = 5m$ (black line), which is accompanied by the emerge of secondary sidebands at $z = 6m$ (red line). Phase-matched four-wave mixing excites further new frequencies ($z = 7m$, blue line). With $\beta_3 = 0.01ps^3/km$ a small asymmetry is induced, apparent by the emerge of the tertiary sidebands in Fig. 1b) (red line). For higher values of β_3 the formation of the spectral sidebands is deferred to higher peak powers or for longer propagation distances and the asymmetry between the red and the blue sidebands grows. The sign of β_3 determines the asymmetry with respect to the red or blue side of the spectrum. A further increase of β_3 leads to a stronger suppression of the

MI, so that the propagation dynamics is overtaken by soliton effects [2].

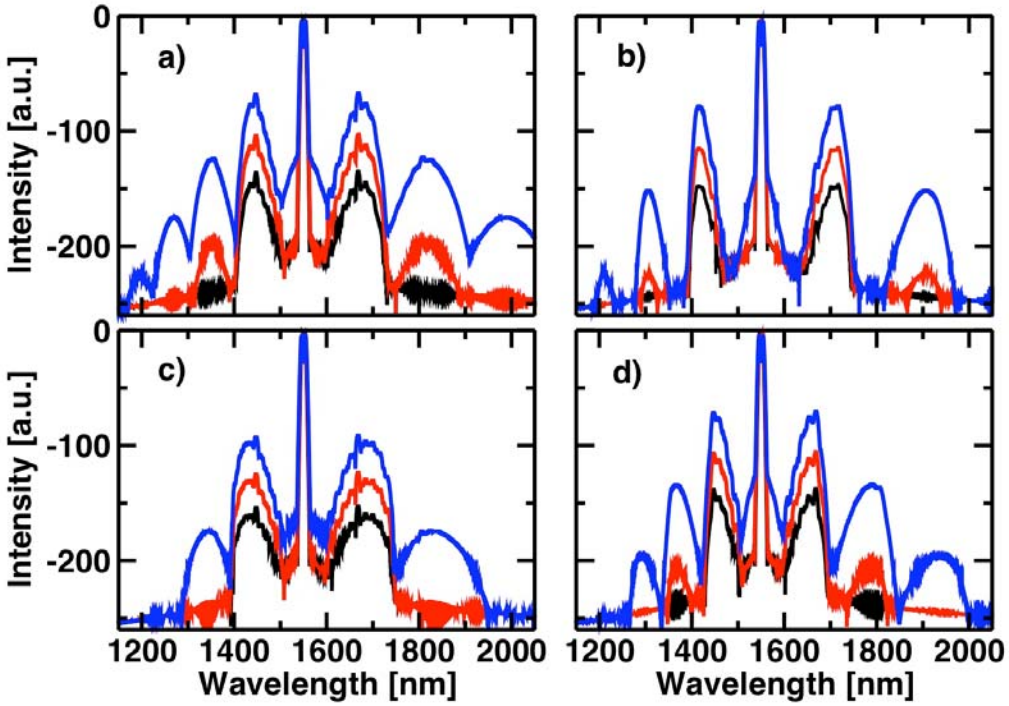

Figure 2: Spectra for the propagation of an input pulse with $P_0 = 0.4kW$ and $\tau_0 = 5ps$ in a HNLF with $\gamma = 10.5W^{-1}km^{-1}$ and $\beta_3 = 0$ after $z = 5m$ (black), $z = 6m$ (red) and $z = 7m$ (blue) for a) $\beta_2 = -1ps^2/km$, $\beta_4 = 0$, b) $\beta_2 = 0$, $\beta_4 = -6\times10^{-4}ps^4/km$, c) $\beta_2 = -1ps^2/km$, $\beta_4 = 6\times10^{-4}ps^4/km$ and d) $\beta_2 = -1ps^2/km$, $\beta_4 = -6\times10^{-4}ps^4/km$.

Contrary to the TOD the shape of a pulse is to a lesser extent affected by FOD, but the critical MI frequency tunes with β_4. Fig. 2 illustrates the evolution of the MI side bands in four different regimes. The emerge and evolution of the side bands is strongest for the case without β_4 (Fig. 2a). For $\beta_2 = 0$ one obtains the critical modulation frequency as $\Omega_c = [48\gamma P_0/|\beta_4|]^{\frac{1}{4}}$, showing that the MI is not only a mechanism which appears in the anomalous dispersion regime (Fig. 2b). Especially in the normal dispersion regime MI gain can appear, which has been demonstrated in [9], and which would be impossible without higher-order dispersion. Beside a change of the position of the sidebands for $\beta_2 = -1ps^2/km$ in addition with a positive or a negative value of β_4, the evolution of the secondary side-lobes by four-wave mixing is dimished (Fig. 2c,d).

2.2 Impact of TOD on soliton propagation

The behavior of a fundamental $N = 1$ soliton under the influence of small TOD term is well known. In first order the soliton phase and velocity are modified, but its shape, amplitude, and width are unchanged. This is accompanied by the excitation of nonsolitonic dispersive radiation at a frequency which is inversely proportional to β_3 [10]. The amplitude of this radiation is exponentially small such that the soliton remains relatively robust [11].
Higher-order solitons are regarded to be less robust with respect to perturbations, such that the propagation is influenced by TOD more strongly. Higher-order solitons are solutions of the NLSE consisting of two or more of the usual fundamental solitons. They are bound when all component solitons propagate with the same velocity and center position. In the presence of perturbations it is believed, that the original bound-state soliton splits always into fundamental solitons and into non-solitonic radiation [1, 12]. Fig. 3 represents the propagation of a bound soliton of order $N = 2.2$ perturbed by the third-order dispersion. For a perturbations with $\beta_3 = 0.01 ps^3/km$ we observe the propagation of a bounded soliton (Fig. 3a) without a breakup into the constituent fundamental solitons. Like in the case $\beta_3 = 0$ for the pure NLSE the pulse is compressed to a fraction of its initial width in the first step of the propagation, followed by an expansion to a pulse with two peaks at $z_0/2$. At the end of the soliton period z_0 the pulse contracts back to the initial shape. This pattern periodically repeats after each section of length z_0. However, due to the presence of β_3 the shape of the pulse becomes asymmetric and the velocity of the bounded soliton is modified. Depending on the sign of β_3 the bounded soliton can propagate slower or faster than the group velocity. The latter is similar to the case of a fundamental soliton and results in a change of the velocity of the whole higher-order soliton. Fig. 3b) shows the corresponding periodic oscillation of the spectrum and the excitation of the resonant radiation frequency. The radiation frequency is located in the normal dispersion regime and is separated from the soliton spectrum. But the periodic oscillation of the spectral width leads to a resonant power transfer to non-solitonic radiation, every time when the soliton spectrum overlaps the resonant frequency of the dispersive wave. By increasing TOD to a value $\beta_3 = 0.03 ps^3/km$ we then observe the well known soliton fission process (Fig. 3 c,d). In the first stage of the propagation the pulse is compressed due to the first step of higher-order soliton dynamics, as explained above. The strong temporal contraction belongs to the maximum expansion of the soliton spectrum. The broadened spectrum in this region touches the resonant radiation frequency of a dispersive wave on the blue side, now located closer to the pump wavelength. At this point a nonsolitonic dispersive wave is generated, which propagates further on with a delayed group velocity. Further propagation now leads to a subsequent break-up of the higher-order soliton into fundamental solitons, which propagate now at different but constant velocities. With increasing N the threshold value of β_3 for SF decreases. This can lead to complicated propagation dynamics as has been observed in supercontinuum generation processes [1]. There, the high-order soliton breaks up into several bounded higher-order solitons having lower values of N, but which are

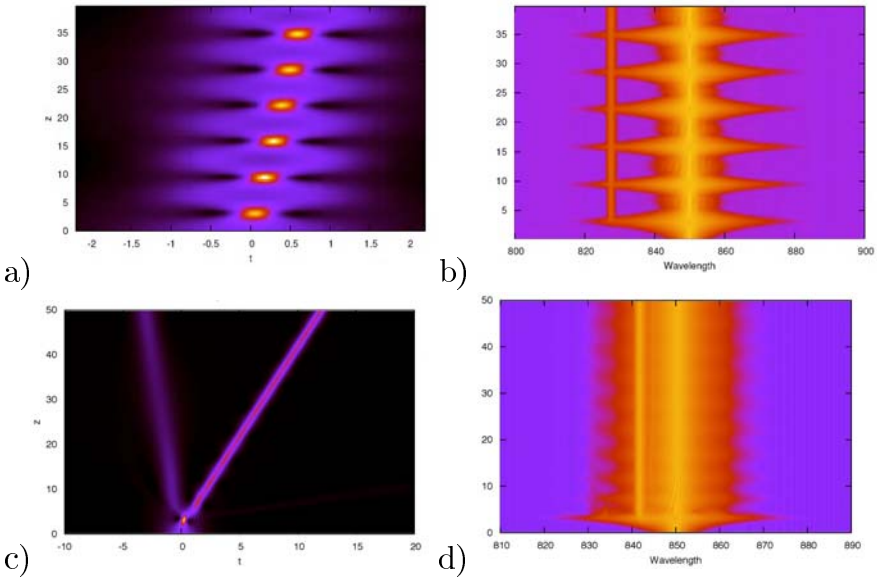

Figure 3: Temporal and spectral propagation of a $N = 2.2$ soliton under the influence of TOD: a,b) Slowing down of a bounded higher-order soliton with $\beta_3 = 0.01ps^3/km$, c,d) Soliton fission with $\beta_3 = 0.03ps^3/km$. In both cases the propagation is associated by the generation of nonsolitonic dispersive radiation. Note the different scaling.

stable for the given value of β_3.

3 Normal dispersion regime

We draw now our attention to the normal dispersion regime ($\beta_2 > 0$), where we do not expect solitonic effects. Fig. 4 represents the simulated pulse shapes and spectra for an injected *sech*-pulse with $\tau_0 = 1.8ps$ and $P_0 = 16W$ in a HNLF with $\beta_2 = 0.2ps^2/km$, $\beta_3 = 0.01ps^3/km$. The pulse shapes show that pulse splitting at the leading edge sets in at $z = 445m$. This pulse-breakup phenomenon in the normal dispersion regime is described in [13, 14]. The TOD leads to an asymmetric temporal development with an enhanced transfer of power from the trailing portion of the pulse to the leading one. A narrow peak builds up and an increase of the peak intensity at the front of the pulse can be observed. The spectrum develops with a small asymmetric broadening towards the blue side. Further propagation as well as a higher peak power leads to a sharp increase of the peak intensity at the front of the pulse, which is halted by temporal pulse splitting. After the splitting a small pedestal on the red side of the spectrum appears. The most important contribution of the TOD in the normal dispersion regime comes from the fact, that the dispersion profile $\beta(\omega)$ merges to the anomalous dispersion regime. Thereby soliton effects add, once the spectrum of the pulse touches the anomalous dispersion regime. Fig. 5 contrasts the propagation in the pure normal dispersion regime $\beta_2 = 0.2ps^2/km$ a),b) with the propagation in addition with $\beta_3 = 0.01ps^3/km$ c),d) and a re-

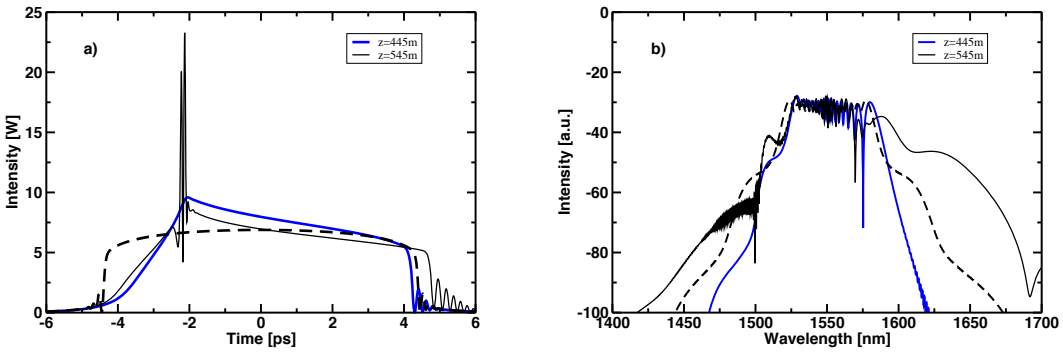

Figure 4: Pulse shapes a) and spectra b) for injected $sech^2$-pulses with $\tau_0 = 1.8ps$ and $P_0 = 16W$ in a fiber with $\beta_2 = 0.2ps^2/km$, $\beta_3 = 0.01ps^3/km$ and $\gamma = 10.5W^{-1}km^{-1}$ after $z = 445m$ (blue) and $z = 545m$ (black). The dashed black lines represent the simulation for the NLSE without TOD.

duced overlap with the anomalous dispersion regime with $\beta_3 = 0.01ps^3/km$ and $\beta_4 = 2\times10^{-4}ps^4/km$, c.f. Fig. 6a. In Fig. 5a,b) the pulse evolves first into a parabolic shape and broadens with further propagation nearly to a rectangular shape, thereby exhibiting optical wave breaking. In this case the spectrum is mainly broadened by self-phase modulation. Introducing TOD (Fig. 5c,d) for the same input pulse leads to the pulse splitting phenomenon. The spectrum is asymmetrically pronounced on the blue side, but also exhibits a broad pedestal on the red side. After the splitting of the pulse the spectrum touches the anomalous dispersion regime (c.f. black curve in Fig. 6a) and the small pedestal on the red side of the spectrum increases with further propagation. This means that more energy is transferred into the anomalous dispersion region, such that soliton effects come into the play, besides the generation of a Stokes component. The further propagation is now additionally determined by soliton fission and by the generation of resonant dispersive waves, leading to a blue shift in the spectrum [3, 2]. To reduce the soliton effects and to suppress the spectral extension on the blue side we narrow the bandwidth of the anomalous dispersion region by switching on a small value of $\beta_4 (= 2 \times 10^{-4}ps^4/km)$ (c.f. blue curve in Fig. 6a). The overall observed behavior (Fig. 5e,f) corresponds to the case $\beta_4 = 0$ described above, up to the point, where the pulse splitting phenomenon occurs. However, now the pulse does not split into fundamental solitons like in Fig. 5c). Also its spectrum extends less to the blue side than in Fig. 5d), but is now more pronounced to the red side. The spectral width saturates after a certain propagation distance and remains in a well bounded domain with a fixed Stokes wavelength, which is located in the anomalous dispersion region. The final spectrum of the pulse is asymmetric with a pronounced red tail and the spectral shape exhibits a depleted region around the ZDW.
Solitons can form only at frequencies within the anomalous dispersion regime, the

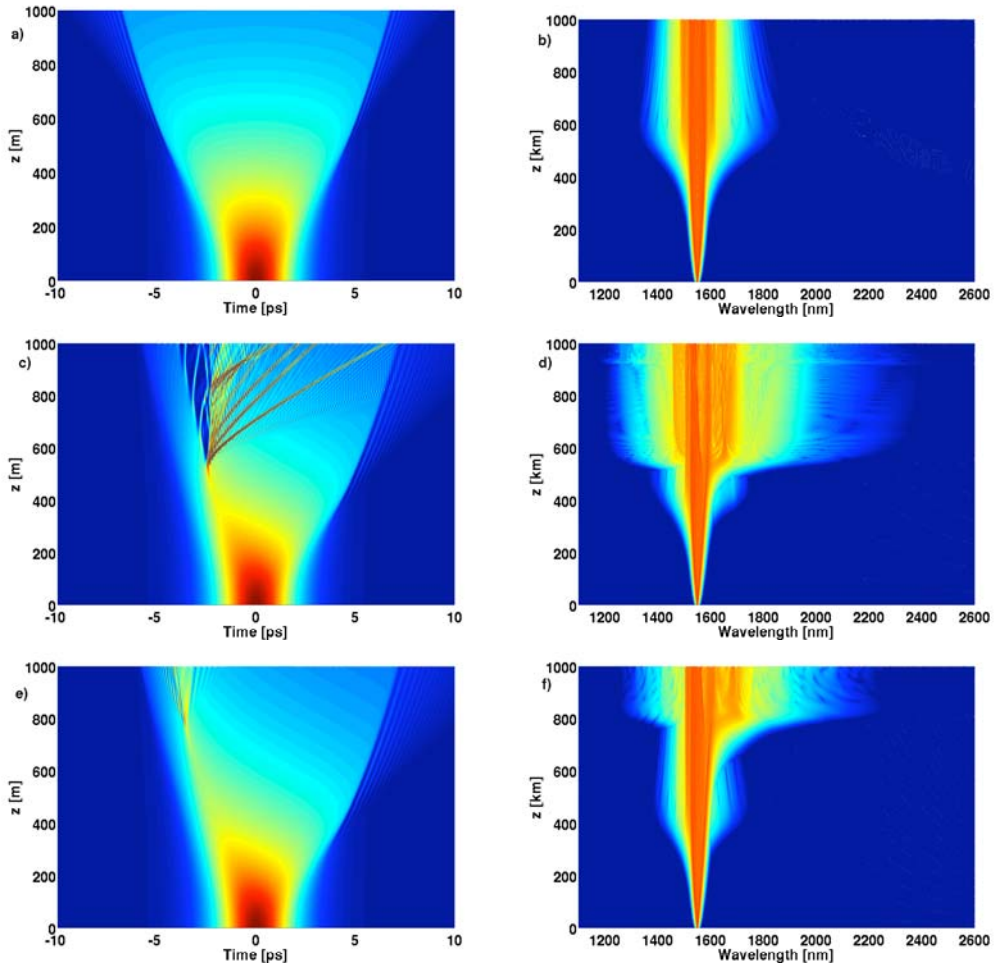

Figure 5: Temporal (left) and spectral (right) evolution of a pulse with $\tau_0 = 1.8ps$ and $P_0 = 16W$ along $1km$ HNLF with $\beta_2 = 0.2ps^2/km$ a,b) $\beta_3 = 0$, $\beta_4 = 0$, c,d) $\beta_3 = 0.01ps^3/km$, $\beta_4 = 0$ and e,f) $\beta_3 = 0.01ps^3/km$, $\beta_4 = 2 \times 10^{-4}ps^4/km$.

bandwidth of which we can reduce by increasing β_4. Fig. 6 represents the behavior by a narrowing of the anomalous regime. Fig. 6a) shows the dispersion profiles for $\beta_4 = 2 \times 10^{-4}ps^4/km$ and $\beta_4 = 3 \times 10^{-4}$ in comparison to the case without β_4. Increasing P_0 leads to a pulse splitting after shorter propagation distances, because the pulse spectrum overlaps earlier with the anomalous dispersion regime, but broadens less to the red side.
Contrary to Raman scattering, where the Stokes component in fused silica is separated by $\approx 13THz$ from the pump frequency, the Stokes component here can be adjusted to an arbitrary wavelength on the red side with an appropriate dispersion profile design.

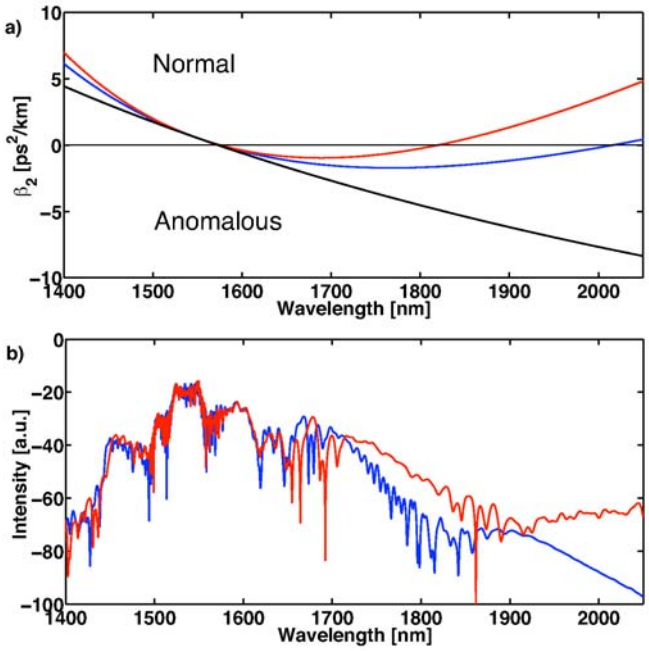

Figure 6: a) Dispersion profiles for $\beta_2 = 0.2ps^2/km$, $\beta_3 = 0.01ps^3/km$, without β_4 (black line) and with small values of β_4: $\beta_4 = 2 \times 10^{-4}ps^4/km$ (blue line), $\beta_4 = 3 \times 10^{-4}ps^4/km$ (red line). b) Spectra at $z = 158m$ and $P_0 = 64W$ for dispersion with $\beta_4 = 2 \times 10^{-4}$ (blue line) and $\beta_4 = 3 \times 10^{-4}$ (red line).

4 Conclusion

By numerically solving the extended nonlinear Schrödinger equation (NLSE) we have investigated the impact of higher-order dispersion on the propagation of optical pulses along highly nonlinear fibers. In the anomalous dispersion regime the modulation instability (MI) and soliton fission (SF) basically modify high-order soliton pulses and their spectra. Third-order dispersion (TOD) can induce SF accompanied by nonsolitonic radiation and yields asymmetric spectra in general, whereas MI is slightly suppressed by TOD in this regime. In the normal dispersion regime the initial spectral broadening of a pulse is dominated by self-phase modulation, whereas its further evolution depends sensitively on the underlying dispersion profile, either allowing for solitonic effects or not. Under presence of TOD pulse splitting has been demonstrated, as well as its suppression later by fourth-order dispersion.

Acknowledgment

The authors acknowledge the support by the projects D14 and D20 in the DFG Research Center MATHEON mathematics for key technologies.

References

[1] Dudley, J.M., Genty, G. and Coen, S.: Supercontinuum generation in photonic crystal fiber. Rev. Mod. Phys., 78, 1135 – 1184 (2006)

[2] Demircan, A. and Bandelow, U.: Analysis of the interplay between soliton fission and modulation instability in supercontinuum generation. Appl. Phys. B, 86, 31 – 39 (2007)

[3] Husakou, A.V. and Herrmann, J.: Supercontinuum generation of higher-order-solitons by fission in photonic crystal fibers. Phys. Rev. Lett., 87, 203901 (2001)

[4] Agrawal, G.P.: Nonlinear Fiber Optics. Academic, San Diego, Calif. (1995)

[5] Coen, S., Chau, A.H.L., Leonhardt, R., Harvey, J.D., Knight, J.C., Wadsworth, W.J. and Russel, P.St.J.: Supercontinuum generation by stimulated Raman scattering and parametric four-wave mixing in photonic crystal fibers. J. Opt. Soc. Am B., 19, 753 – 764 (2002)

[6] Demircan, A. and Bandelow, U.: Supercontinuum generation by the modulation instability. Opt. Comm., 244, 181–185 (2005)

[7] Calvacanti, S.B.,Cressoni, J.C., Da Cruz, H.R., and Gouveia-Neto, A.S.: Modulation instability in the region of minimum group-velocity dispersion of single-mode optical fibers via an extended nonlinear Schrödinger equation. Phys. Rev. A, 43, 6162–6165 (1991)

[8] Nakazawa, N., Suzuki, K., Kubota, H. and Haus, H.A.: Higher-order solitons and the modulation instability. Phys. Rev. A, 39, 5768–5776 (1989)

[9] Reeves, W.H., Skryabin, D.V., Biancalana, F., Knight, J.C., Russel, P.St.J., Omenetto, F.G., Efimov, A. and Taylor, A.J.: Transformation and control of ultra-short pulses in dispersion-engineered photonic crystal fibres. Nature, 424, 511–515 (2003)

[10] Wai, P.K.A., Chen, H.H. and Lee, Y.C.: Radiations by solitons at the zero group-dispersion wavelength of single-mode optical fibers. Phys. Rev. A., 41, 426–439, (1990)

[11] Kuehl, H.H. and Zhang, C.Y.: Effects of higher-order dispersion on envelope solitons. Phys. Fluids, 2, 889–900 (1990)

[12] Friberg S.R. and DeLong, K.W.: Breakup of bound higher-order solitons. Opt. Lett., 17, 979–981, (1992)

[13] Demircan, A., Kroh, M., Bandelow, U., Hüttl, B. and Weber, H.G.: Compresion limit by third-order dispersion in the normal dispersion regime. IEEE Phot. Tech. Lett., 18, 2353–2355 (2006)

[14] Demircan, A. and Bandelow, U.: Limit for pulse compression by pulse splitting. Opt. Quant. Elect., 38, 1167–1172 (2006)

[15] Gaeta, A.L.: Nonlinear propagation and continuum generation in microstructured optical fibers. Opt. Lett., 27, 924–926 (2002)